Preparation of a Heterogeneous Hollow-Fiber Affinity Membrane Modified with a Mercapto Chelating Resin

Bing Wang, Lei Huang, Feng Xiao, Wei Liu, Xipeng Jiang

Key Laboratory of Hollow-Fiber Membrane Materials and Membrane Processes of the Ministry of Education, School of Materials Science and Chemical Engineering, Tianjin Polytechnic University, Tianjin 300160, People's Republic of China

Received 11 September 2006; accepted 23 December 2006
DOI 10.1002/app.26351
Published online 25 April 2007 in Wiley InterScience (www.interscience.wiley.com).

ABSTRACT: A high-quality, heterogeneous hollow-fiber affinity membranes modified with mercapto was prepared through phase separation with blends of a chelating resin and polysulfone as membrane materials, poly(ethylene glycol) as an additive, *N,N*-dimethylacetamide as a solvent, and water as an extraction solvent. The effects of the blending ratio and chelating resin grain size on the structure of the hollow-fiber affinity membrane were studied. The effects of the composition of the spin-cast solution and process parameters of dry–wet spinning on the structure of the heterogeneous hollow-fiber affinity membrane were investigated. The pore size, porosity, and water flux of the hollow-fiber affinity membrane all decreased with an increase in the additive content, bore liquid, and dry-spinning distance. With an increase in the extrusion volume outflow, the external diameter, wall thickness, and porosity of the hollow-fiber affinity membrane all increased, but the pore size and water flux of the hollow-fiber affinity membrane decreased. It was also found that the effects of the internal coagulant composition and external coagulant composition on the structure of the heterogeneous hollow-fiber affinity membrane were different. The experimental results showed that thermal drawing could increase the mechanical properties of the heterogeneous hollow-fiber affinity membrane and decrease the pore size, porosity, and water flux of the heterogeneous hollow-fiber affinity membrane, and the thermal treatment could increase the homogeneity and stability of the structure of the heterogeneous hollow-fiber affinity membrane. © 2007 Wiley Periodicals, Inc. J Appl Polym Sci 105: 1687–1699, 2007

Key words: blends; chromatography; membranes; resins; phase separation; separation techniques

INTRODUCTION

An affinity filter membrane integrates the advantages of both affinity chromatography and modern membrane techniques and can be used to treat industrial wastewater and recover metal ions.[1–6] An affinity filter membrane with definite millipores has an affinity agent on its inner and outer surfaces as a carrier of the affinity agent. When a fluid is filtered through the membrane, the object products will quickly combine with the relevant functional groups of the affinity agent. The products sorbed on the membrane will soon be desorbed when an eluent passes through the membrane. Consequently, the separation period is short, and the coefficient of the affinity functional groups' use is substantial. In addition, because the membrane has good properties of fluid transfer, mechanical stability, and low operating pressure for the equipment, the process engineering is apt to be magnified. Mercury metal, inorganic mercury salt, and organic mercury compounds can negatively affect a person's health. After inhalation into the human body, mercury vapor can be accumulated easily in the central nervous system, liver, and kidneys. In the bloodstream, mercury ions can firmly combine with proteins in nephrocytes, thus causing destruction of kidney function. Organic mercury compounds are apt to dissolve in fat and accumulate in the human body. In our previous study,[7] an amidophosphoric acid resin was used as a carrier of a chelating affinity agent and blended with polysulfone (PSF) to prepare a new type of heterogeneous plate affinity filter membrane for the removal of Hg^{2+}, and the greatest chelating capacity of Hg^{2+} that could be reached was 1050 μg/cm^2 of the membrane. As everyone knows, the loadability of the unit volume of a hollow-fiber membrane surface is much larger than that of a plate membrane, and the intensity of a hollow-fiber membrane is hard enough to support itself, whereas that of a plate membrane is not. Thus, there is both theoretical and practical significance in studying the preparation of a heterogeneous hollow-fiber affinity membrane modified with a mercapto chelating resin for the recovery of Hg^{2+}, based on a chelating plate membrane, and the

Correspondence to: B. Wang (bingwang666@yahoo.com.cn).

Contract grant sponsor: Natural Science Foundation of Tianjin; contract grant number: 05YFJMJC04200.

greatest chelating capacity of the hollow-fiber affinity membrane for Hg^{2+} was 1090 μg/cm^2 of the membrane under the appropriate conditions.

EXPERIMENTAL

Materials and reagents

The mercapto chelating resin (D190) used in this study was supplied by Nankai University Chemical Plant (China), PSF (intrinsic viscosity = 0.57) was obtained from Shanghai Shuguang Chemical Plant (Shanghai, China), and *N*,*N*′-dimethylacetamide (DMAc) was obtained from Tianjin Chemical Reagent Plant (Tianjin, China). Poly(ethylene glycol) (PEG; number-average molecular weight = 10,000) was obtained from Tianjin Chemical Reagent Plant.

Main apparatuses

An XL30 environmental scanning electron microscope was acquired from Philips (Holland). An HD-201 electronic strand strength meter was obtained from Hongda Laboratory Apparatus, Ltd. (Sichuang, China). The dry–wet-spinning equipment was made by Tianjin Polytechnic University (Tianjin, China).

Preparation of the spin-cast solution

Some PSF and PEG (or NH_4Cl) were dissolved in DMAc to form a PSF solution of a certain concentration. Then, the quantitative mercapto chelating resin (D190), which was ground and sifted, was put into the PSF solution, and the solution of D190 and PSF was rigorously stirred for 8 h. Because the D190 could not be dissolved in DMAc, the solution of D190 and PSF was heterogeneous. A certain composition of the heterogeneous D190/PSF spin-cast solution could be obtained after vacuum deaeration.

Preparation of the heterogeneous hollow-fiber affinity membrane modified with the mercapto chelating resin

The dry–wet-spinning method was adopted to prepare the heterogeneous hollow-fiber affinity membrane in the spinning equipment. The spin-cast solution was put into the storage tank and deaerated under negative pressure. High-pressure nitrogen was used as the pressure source to push out the spin-cast solution, which was measured from the spinning head; at the same time, the core liquid went from the central cavity of the spinning head into the hollow-fiber cavity as its supporter and inner coagulum medium under the pressure of the head tank. Lastly, the spinning dope went away from the spinning head, passing the air clearance between the spinning head and coagulating bath tank into the coagulating bath tank; when it had coagulated into the mold completely, by heat-drawing and heat-setting treatments, the heterogeneous hollow-fiber affinity membrane modified with the mercapto chelating resin was prepared. The heterogeneous hollow-fiber affinity membrane modified with the mercapto chelating resin should be preserved in a hygrometric state.

Measurement of the mechanical properties of the hollow-fiber affinity membrane

The mechanical property measurements were preformed with an HD-201 electronic strand strength meter, and the given length of the sample was 500 mm. All the tensile data obtained were average values of at least three measurements.

Environmental scanning electron microscopy (ESEM) of the hollow-fiber affinity membrane

The heterogeneous hollow-fiber affinity membrane modified with the mercapto chelating resin was immersed in 50% aqueous glycerol for 24 h. Then, the membrane was taken out, and the glycerol on its surfaces was wiped away. The membrane was dehydrated stepwise by mass fractions of 50, 70, 90, and 100% ethanol sequentially. The ESEM characterization was performed on a coating film by ion sputtering after the membrane was frozen in liquid nitrogen and fastened onto the sample table, and the thickness was about 20 nm. The pore size and size distribution of the membrane were obtained from the observation of the morphological structure of the cross section of the heterogeneous hollow-fiber affinity membrane modified with the mercapto chelating resin with an XL30 environmental scanning electron microscope.

Measurement of the water flux of the hollow-fiber affinity membrane

A schematic diagram of the experimental apparatus for the measurement of the water flux is shown in Figure 1. The heterogeneous hollow-fiber affinity membrane modified with the mercapto chelating resin was installed on the self-made hollow-fiber membrane module, and when the pure water permeated from the outside into the inside of the membrane under a given pressure of the circulating pump, the pure water volume through the given membrane area was noted at the given time. The water flux was calculated as follows:

$$Q = \frac{V}{St} \tag{1}$$

where Q is the flux (L/m^{2}h), V is the volume of the permeate liquid (L), S is the effective membrane area of the hollow-fiber membrane, and t is the ultrafiltration time (s).

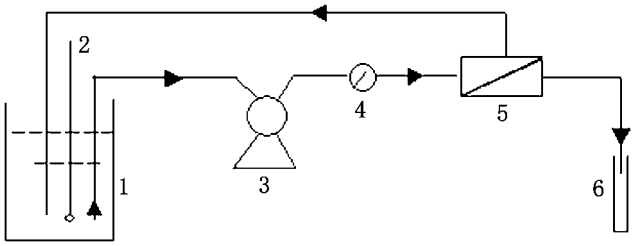

Figure 1 Schematic diagram of the retention measurement apparatus for the membrane: (1) reservoir, (2) thermometer, (3) water pump, (4) barometer, (5) plate membrane module, and (6) volumetric cylinder.

Measurement of the porosity of the hollow-fiber affinity membrane

The experiment was carried out by the gravimetric method, and glycerol was used as the soaking solution of the hollow-fiber membrane.[8] A piece of a given area (S) of the hygrometric-state hollow-fiber membrane was sheared and weighed [wet weight (W_w)] after glycerol was wiped from the membrane surface, then the membrane was dried in a vacuum-drying oven to a constant weight [dry weight of the membrane (W_d)], and the porosity was calculated as follows:

$$P_r = \frac{W_w - W_d}{Sd\rho} \times 100\% \quad (2)$$

where d is the average thickness of the membrane and ρ is the glycerol density.

Measurement of the pore size of the hollow-fiber affinity membrane

The pore size of the heterogeneous hollow-fiber affinity membrane modified with the mercapto chelating resin was determined by the filtering velocity method.[8] The membrane pore diameter (r_f) was calculated as follows:

$$r_f = \sqrt{\frac{8 \times (2.90 - 1.75P_r)\mu LQ}{P_r \Delta PS}} \quad (3)$$

where P_r is the porosity, L is the membrane thickness, μ is the viscosity of the permeate liquid, Q is the water flux, ΔP is the pressure, and S is the permeated area.

RESULTS AND DISCUSSION

ESEM of the hollow-fiber affinity membrane with different contents of the chelating resin

Figure 2 presents the environmental spinning electrical graph of the heterogeneous hollow-fiber affinity membrane with different contents of the chelating resin. The membrane structure close to the two surfaces was entirely a fingerlike, pore-size structure, and there was a thin, compact, spongeous structure between the two loose layers. Such a membrane structure was due to the diffusivity of the solvent DMAc of the spinning dope in the dry- and wet-spinning process. In this study, the fiber-spinning process was adopted from dry–wet-spinning technology. In the stage of dry spinning, the internal and external surfaces of the spinning dope were all in different media, and the external surface was in air. Because the solvent DMAc was easy to volatilize and the speed was a

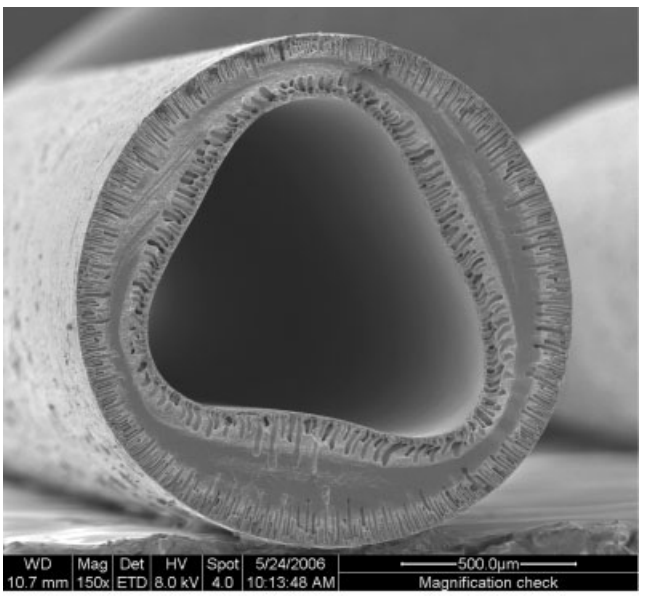

(a)

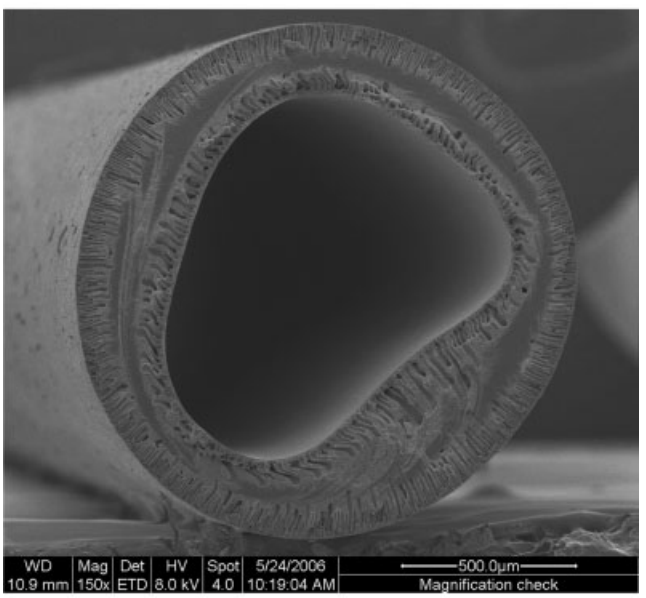

(b)

Figure 2 ESEM of cross sections of the heterogeneous hollow-fiber affinity membrane with different contents of the chelating resin: (a) 6 and (b) 8%.

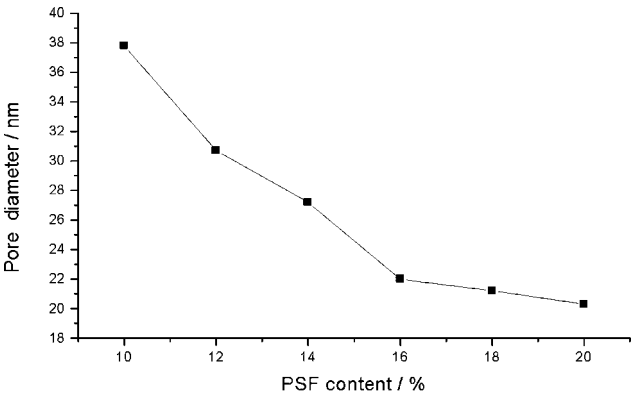

Figure 3 Relationship between the PSF content and pore diameter of the hollow-fiber affinity membrane. The additive content was 0%, the casting solution temperature was 25°C, the coagulating bath temperature was 25°C, and the ultrafiltration pressure was 0.1 MPa.

little slower, the diffusivity of the solvent from the spinning dope to the external surface could form a fingerlike, pore-size structure in the external surface. Although the internal surface fully in contact with the core liquid, the solvent DMAc on the internal surface was totally mixed with water, so the solvent in the spinning dope could diffuse to the core liquid, and this resulted in the concentration of PSF close to the external surface and formed a fingerlike, pore-size structure. In the wet-spinning stage, the internal and external surfaces were all dipped in the coagulating bath; therefore, the solvent in the spinning dope began to diffuse to the external coagulation bath and to the core liquid at the same time. No matter where the solvent in the center of the membrane diffused, the resistance was much more. This was the reason for the formation of the rich phase of the polymer PSF in the membrane and the appearance of the phase separation. To delay the liquid–liquid delamination, the membrane structure forming in the membrane was a compact, spongeous structure.

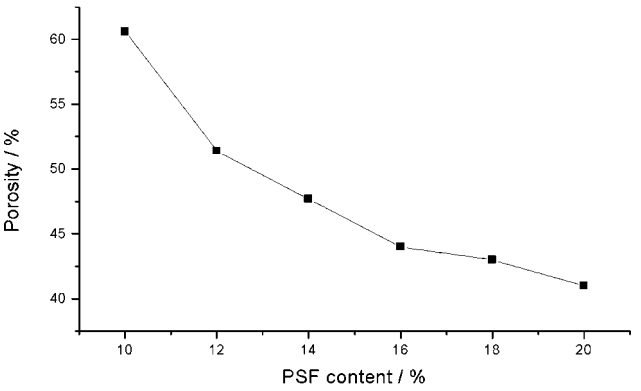

Figure 4 Relationship between the PSF content and porosity of the hollow-fiber affinity membrane. The additive content was 0%, the casting solution temperature was 25°C, the coagulating bath temperature was 25°C, and the ultrafiltration pressure was 0.1 MPa.

TABLE I
Effects of the Additive PEG Concentration on the Structure of the Hollow-Fiber Affinity Membrane

PEG content (%)	Water flux (L/m^2 h)	Pore diameter (nm)	Porosity (%)
0	40.1	24.0	47.2
2	168.0	34.1	59.1
4	179.6	37.2	61.2
6	190.1	38.5	62.1
8	201.7	40.2	64.4
10	205.3	43.4	68.7

The additive was PEG (molecular weight = 10,000), the casting solution temperature was 25°C, the coagulating bath temperature was 25°C, and the ultrafiltration pressure was 0.1 MPa.

Effects of the contents of the PSF and additive on the structure of the hollow-fiber affinity membrane

Figure 3 shows the effect of the concentration of PSF on the pores of the hollow-fiber affinity membrane, and Figure 4 shows the effect of the concentration of PSF on the porosity of the hollow-fiber affinity membrane. The concentration of PSF, which was the main material composing the pore structure, affected the morphological structure of the hollow-fiber affinity membrane directly. Figures 3 and 4 show that both the pore size and the porosity decreased with the increase in the PSF concentration in the spin-cast solution. With the increase in the PSF concentration, the liquid–liquid phase separation appeared under the skin layer in the process of preparation for the hollow-fiber affinity membrane in the dry–wet-spinning technology. Because the number of the crystal nucleus in the poor phase of PSF increased, the network structure formed by the crystal nucleus after desolventizing became more compact, and as the pore size became

TABLE II
Effects of the Chelating Resin Content on the Structure of the Hollow-Fiber Affinity Membrane

Resin content (%)	Water flux (L/m^2 h)	Pore diameter (nm)	Porosity (%)
0	41.0	4.9	79.0
2	39.0	5.7	78.1
4	60.0	23.1	65.3
6	180.0	28.9	61.3
8	200.0	51.0	60.2
10	207.0	52.4	55.3

The chelating resin grain diameter was 97–105 μm, the additive was PEG (molecular weight = 10,000), the casting solution temperature was 25°C, the coagulating bath temperature was 25°C, and the ultrafiltration pressure was 0.1 MPa.

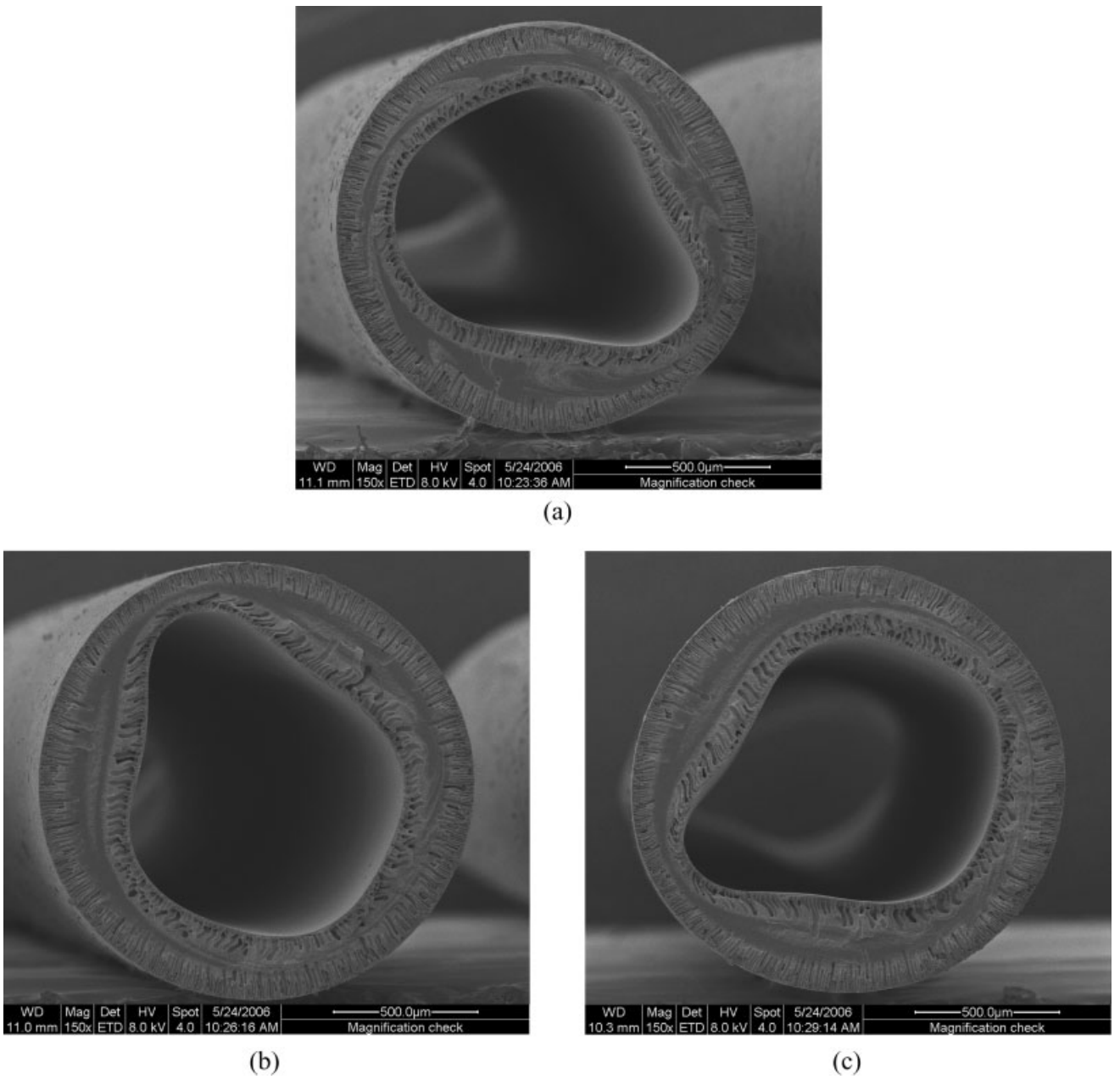

Figure 5 ESEM of cross sections of the hollow-fiber affinity membranes with different chelating resin grain diameters: (a) 74–88, (b) 97–105, and (c) 125–147 μm.

smaller, the porosity decreased, and the flux was reduced. Meanwhile, the PSF concentration affected the spinning dope directly, and too much or too little viscosity of the spinning dope resulted in an unstable spinning dope and affected the structure and performance of the hollow-fiber membrane. When the spincast solution went off the spinning head and came into contact with the coagulating bath, it first formed compact surface layers like a spongeous structure on both the internal and external surfaces of the membrane. However, because the stress that was applied when the polymer was desolventized and compacted could not completely disappear through the creep of the polymer, the compact surface layer broke at the stress rookery, and this breakpoint was the growing point of the fingerlike pores. As soon as the fingerlike pores appeared at the breaking point, they grew up to the membrane matrix from this point. The exchange rate of the solvent and the coagulator could be changed by the adjustment of the content of the additive PEG (molecular weight = 10,000); that is, the stress state of the membrane surface in the gel process of the as-formed fiber changed. In this way, the goal of controlling the pore size of the membrane and the degree of growth in the membrane matrix was obtained. Table I shows the effect of the concentration

of the additive PEG (molecular weight = 10,000) on the structure of the hollow-fiber affinity membrane. The average pore size of the membrane became larger and the porosity also showed an upward trend with the increase in the content of the additive PEG (molecular weight = 10,000), and the water flux increased under the combined effects of the pore size and porosity. When the content of PEG in the spinning liquid increased, the exchange rate of the solvent and the precipitant was expedited for the strong hydrophilic effect, and many more fingerlike pores formed. The increase in the proportion of the fingerlike pores appeared with the increase in the porosity and pore size. However, too much additive reduced the intensity of the membrane, and so the viscosity of the spinning liquid was too high for spinning.

Effects of the chelating resin content on the structure of the hollow-fiber affinity membrane

Changes in the structure of the hollow-fiber membrane with the chelating resin content are shown in Table II. Around 2%, the water flux and pore size were less, the porosity was greater, and the effect of the chelating resin content on the structure of the hollow-fiber affinity membrane was negligible. In the low-concentration region, the content of the chelating resin was less. Thus, in the process of phase inversion, the membrane pores appeared mainly in the continuous phase of PSF. First, the PSF macromolecules gathered together, formed the concentrated phase, and became an island structure. The parts among the islands formed the dilute phase. With the solvent (DMAc) diffusion, the concentration phase formed the dense parts of the hollow-fiber affinity membrane, and the dilute phase formed the pores of the hollow-fiber affinity membrane. The size of the pores could be controlled by the speed of the phase inversion. The pore diameter of the hollow-fiber membrane changed suddenly from several nanometers to tens of nanometers when the content of the chelating resin increased to 4%. This means that the mechanism of pore formation changed. The chelating resin and PSF formed the heterogeneous hollow-fiber membrane and had partial compatibility. With the increase in the content of the chelating resin, the degree of phase separation increased, and the nanopore diameters increased among the chelating resin phases and PSF phases. When the content of the chelating resin was greater than 4%, the trend of gathering chelating resin macromolecules could be enhanced, the phases separated significantly, and the nanopore diameters between the two phases increased; thus, the water flux also increased with them. However, the number of nanopores decreased per unit of volume, and the porosity decreased, too.

Effects of the chelating resin size on the structure of the hollow-fiber affinity membrane

Figure 5 shows scanning electron micrographs of the cross sections of hollow-fiber affinity membranes with different chelating resin grain sizes and additionally shows that the pores of the hollow-fiber membranes underwent an obvious change with different sizes of the chelating resin grains. When the chelating resin grain diameter was 97–105 μm, the pores of the hollow-fiber membrane were largest. When the chelating resin grain diameter was 125–147 μm, the pores of the hollow-fiber affinity membrane were larger; when the chelating resin grain diameter was 74–88 μm, the pores of the hollow-fiber membranes were normal. Table III shows the changes in structure of the hollow-fiber membrane with chelating resin grains of different sizes. With the decreasing size of the chelating resin grains, the water flux and pores size increased first and decreased later. This was related to the interface sorption between the chelating resin and casting solution. Chelating resin grains simultaneously adsorbed PSF and DMAc. With the decrease in the size of the chelating resin grains and the increase in the interface energy, the adhesion increased between the chelating resin and PSF solution, and the size of the interface pores decreased. With the diffusion of the solvent (DMAc), the macromolecules had more of a chance to gather and form more colloid network structures when the hollow-fiber membrane was prepared with the phase-inversion method. Thus, the ratio of the larger gathering pores and porosity of the hollow-fiber affinity membrane increased. Meanwhile, the degree of both connections increased with the decrease in the size of the chelating resin grains. When the PSF macromolecules assembled in the coagulation bath, they drove the chelating resin grains to move, forming larger pores and increasing the water flux.

Effects of the temperature of the spin-cast solution on the structure of the hollow-fiber affinity membrane

Changes in the structure of the hollow-fiber affinity membrane with the temperature of the spin-cast solution

TABLE III
Effects of the Chelating Resin Size on the Structure of the Hollow-Fiber Affinity Membrane

Grain diameter (μm)	Water flux (L/m^2 h)	Pore diameter (nm)	Porosity (%)
125–147	120.1	30.1	60.1
97–105	130.2	39.1	47.0
74–88	50.0	20.1	49.1

The chelating resin grain content was 6%, the additive was PEG (molecular weight = 10,000), the casting solution temperature was 25°C, the coagulating bath temperature was 25°C, and the ultrafiltration pressure was 0.1 MPa.

TABLE IV
Effects of the Spin-Cast Solution Temperature on the Structure of the Hollow-Fiber Affinity Membrane

Temperature (°C)	Water flux (L/m^2 h)	Pore diameter (nm)	Porosity (%)
20	140.1	42.3	65.3
25	135.3	40.1	64.1
30	130.4	38.1	62.6
35	123.1	36.2	61.9
40	119.8	35.4	61.1

The additive was PEG (molecular weight = 10,000), the PEG concentration was 4%, the coagulating bath temperature was 25°C, and the ultrafiltration pressure was 0.1 MPa.

are shown in Table IV. The increase in the temperature resulted in the decrease in the viscosity of the spinning liquid, and when the spinning liquid was immersed in the coagulation bath, the double diffusion rate of the solvent and the coagulator increased, and consequently, the flux, pore size, and porosity of the hollow-fiber affinity membrane increased. What needs to be explained is the conclusion that the increase in the spinning liquid favorable for the increase in the membrane flux is applicable only within limits. Too high a temperature will lead to solvent volatilization promptly, and a compact membrane will be formed instead. Dry spinning is an extreme example of such a case. A hollow-fiber membrane with good water permeability can also be obtained at a lower spinning temperature and a lower whole solid concentration. Therefore, the spinning temperature and concentration can be adjusted within limits.

Effects of the extrusion rate on the structure of the hollow-fiber affinity membrane

Table V shows the effects of the volume flow rate of the extrusion on the hollow-fiber affinity membrane structure under other constant spinning conditions, such as the dry-spinning line, the reeling velocity, and the flow rate of the core liquid. In the spinning process of the hollow-fiber affinity membrane, the factors that affect the quality and structure of the hollow-fiber affinity membrane can be divided into two parts. One is the effect of the composition of the spinning dope, such as the composition and dosage of the additives, and the content of the polymer. The other is the effect of the process conditions, such as the reeling velocity, the temperature of the spinning liquid, the pressure in the spinning process, the proportioning and temperature of the core liquid, the temperature of the coagulating bath, and the distance of the vaporing part. Both factors have restrictions and are related to each other in the experimental and product procedures.

Table V shows that when the volume flow rate increased, the external diameter, wall thickness, and porosity of the hollow-fiber affinity membrane increased, whereas the pore size and flux decreased. The continuity condition of the spinning process is as follows:[9]

$$\rho\pi(R^2 - r^2)V = \rho\pi(R_0^2 - r_0^2)V_0 \quad (4)$$

where R and r are the external and internal diameters of the hollow-fiber membrane, respectively; R_0 and r_0 are the external and internal diameters of the spinning head, respectively; ρ is the density of the jetting spinning dope; and V_0 and V are the extrusion rate and movement velocity of the spinning dope, respectively. When the extrusion speed increases and the movement velocity of the spinning dope remains invariable to meet the continuity condition, the left-hand-side term of eq. (4) [$\pi(R^2 - r^2)$] increases' that is, the wall thickness of the hollow-fiber membrane increases. Because the core liquid and the flow rate are constant, the internal diameter of the hollow-fiber membrane remains unaltered, and the external diameter of the hollow-fiber membrane increases. The changes in the flux, pore size, and porosity of the hollow-fiber membrane are consistent with the results in the literature; that is, the water flux decreases with the increase in the wall thickness of the hollow-fiber membrane. The reason for the pore size decreasing was the increase in the shearing rate, which caused the volume flow rate when the polymer PSF solution flowed in the spinning head. The increase in the shearing stress could enhance the degree of orien-

TABLE V
Effects of the Extrusion Volume Outflow on the Structure of the Hollow-Fiber Affinity Membrane

Extrusion volume outflow (mL/min)	External diameter (mm)	Wall thickness (mm)	Water flux (L/m^2 h)	Pore diameter (nm)	Porosity (%)
10	1.20	0.23	130.1	41.2	62.1
20	1.27	0.25	121.2	39.0	64.0
30	1.41	0.27	118.7	37.1	67.1
40	1.50	0.30	111.6	36.3	68.3

The dry-spinning distance was 10 cm, the additive was PEG (molecular weight = 10,000), the PEG concentration was 4%, the coagulating bath temperature was 25°C, and the ultrafiltration pressure was 0.1 MPa.

TABLE VI
Effects of the Bore Liquid Outflow on the Structure of the Hollow-Fiber Affinity Membrane

Bore liquid outflow (L/h)	External diameter (mm)	Inner diameter (mm)	Wall thickness (mm)	Water flux (L/m^2 h)	Pore diameter (nm)	Porosity (%)
0.45	1.25	0.68	0.28	121.3	39.1	64.0
0.50	1.28	0.72	0.27	134.1	42.1	68.1
0.55	1.40	0.91	0.24	140.2	46.4	70.2
0.60	1.47	1.0	0.19	148.1	50.0	74.3

The extrusion volume outflow was 20.4 mL, the additive was PEG (molecular weight = 10,000), the PEG concentration was 4%, the coagulating bath temperature was 25°C, and the ultrafiltration pressure was 0.1 MPa.

tation of the molecular chain of the PSF to make the array more compact and lead to the increase in the average pore size of the hollow-fiber membrane.

Effects of the flow rate of the core liquid on the hollow-fiber affinity membrane

The inset tube-type spinning head of the hollow fiber was adopted; the core liquid was passed over the inset tube to offer inside support for the fiber that just extruded and to produce the inside coagulation effect. The effect of the flow rate of the core liquid on the structure of the hollow-fiber membrane is shown on Table VI. With the increase in the flow rate of the core liquid, the internal and external diameters both increased, but the increase in the internal diameter was faster, the wall thickness of the hollow fiber decreased, and the flux, pore size, and porosity increased. The reason is that with the increase in the flow rate of the core liquid, the acting force of the core liquid on the inner wall increased, and that resulted in the decrease in the wall thickness of the spinning dope; meanwhile, the increase in the flow rate of the core liquid increased the diffusion velocity of the solvent in the spinning dope to the core liquid and increased the differential concentration between the solvent and the coagulator on the interface of the membrane. Then, the rate of the membrane formation was quickened, and the porosity, pore size, and flux increased. However, with the increase in the flow rate of the core liquid, the internal and external diameters of the membrane increased, then the wall thickness decreased rapidly, and the bearing capacity of the membrane decreased suddenly.

TABLE VII
Effects of the Internal Coagulant Composition on the Structure of the Hollow-Fiber Affinity Membrane

DMAc content (%)	Water flux (L/m^2 h)	Pore diameter (nm)	Porosity (%)
2	184.1	40.1	68.1
4	179.2	37.2	61.3
6	171.3	35.4	56.1
8	162.6	33.4	51.1
10	154.3	31.2	48.2

The evaporation time was 10 s, the additive was PEG (molecular weight = 10,000), the PEG concentration was 4%, the casting solution temperature was 25°C, the coagulating bath temperature was 25°C, and the ultrafiltration pressure was 0.1 MPa.

Effects of the coagulating conditions on the structure of the hollow-fiber affinity membrane

Table VII shows the effects of the DMAc content in the inner coagulator on the structure of the hollow-fiber membrane. The coagulation of the hollow fiber included two parts: inner coagulation by the effect of the core liquid and outer coagulation by the effect of the coagulation liquid. The inner coagulating liquid, namely the core liquid, was a mixed liquid of the solvent DMAc and the coagulator H_2O.

The effect of the content of DMAc in the outer coagulator on the structure of the hollow-fiber membrane is shown in Table VIII. Under the same conditions of the outer coagulating condition, with the increase in the solvent DMAc content in the inner coagulating liquor, the coagulating conditions were alleviated, the membrane structure became more compact, and the flux, pore size, and porosity decreased. Table VIII shows that the flux, pore size, and porosity had a minimum with the change in the content of DMAc in the coagulating liquid. The reason is that when the con-

TABLE VIII
Effects of the External Coagulant Composition on the Structure of the Hollow-Fiber Affinity Membrane

DMAc content (%)	Water flux (L/m^2 h)	Pore diameter (nm)	Porosity (%)
2	184.2	40.1	68.1
4	173.1	38.2	66.4
6	170.2	37.2	63.2
8	165.5	33.5	59.1
10	158.4	31.4	57.0
12	161.2	32.8	58.8

The internal coagulant composition was 2% DMAc, the evaporation time was 10 s, the additive was PEG (molecular weight = 10,000), the PEG concentration was 4%, the casting solution temperature was 25°C, the coagulating bath temperature was 25°C, and the ultrafiltration pressure was 0.1 MPa.

tent of the solvent DMAc in the outer coagulating liquid increased, the forming conditions were gradually alleviated, the rate of the double diffusion decreased, the membrane structure was more compact, and the flux, pore size, and porosity decreased; when the content of the solvent DMAc in the coagulating bath increased continually, the structure of the membrane became loose again for the swelling effect of the solvent DMAc on the PSF, and then the flux, pore size, and porosity increased a little.

Effects of the length of the dry-spinning line on the structure of the hollow-fiber affinity membrane

In the spinning process, the stresses applied on the spinning dope were mainly the following ones: the extensional force (F_t) forced by the collecting device on the spinning dope, the deadweight (F_g) of the spinning dope, the inertia force (F_{in}) making the spinning accelerate, the friction force (F_f) caused by the spinning dope and surrounding medium, the surface tension (F_s) of the spinning dope, and the rheological resistance (F_R) of the intermolecular chains in the spinning dope. The acting forces of any point in the spinning dope satisfied the equilibrium of these forces:

$$F_t + F_g = F_R + F_S + F_f + F_{in} \tag{5}$$

The exterior tension (F_t) caused by the winding equipment at L away from the spinning head can be expressed as follows:[10]

$$F_t = P^0_{xx}(L) \cdot \pi R_L^2 \tag{6}$$

where P^0_{xx} is the winding stress. The equation of the gravity (F_g) can be expressed as follows:[10]

$$F_g = (L - L_0)\pi R_L^2 g\left(1 - \frac{\rho^0}{\rho}\right)\cos\omega \tag{7}$$

The cos ω value is relatable to the direction of the motion. When the direction of spinning is vertically upward, cos ω = −1; when it is horizontal, cos ω = 0; and when it is vertically downward, cos ω = 1. In this study, the direction of the spinning in the dry-spinning stage is downward vertically, and so cos ω = 1. ρ^0 is the density of the medium, and ρ is the density of the spinning dope. F_{in} makes the spinning accelerate. The work applied by the outside forces on the spinning dope equals the increase in its kinetic energy, and it can be calculated with the following equation:

$$\begin{aligned} F_{in}(X_2 - X_1) &= \frac{1}{2g}(mv_2^2 - mv_1^2) \\ F_{in}\Delta X &= \frac{m(v_2^2 - v_1^2)}{2g} \end{aligned} \tag{8}$$

where X_1 and X_2 are the distances of the two points on the nozzle plate, respectively; v_1 and v_2 represent the movement velocities when the spinning dope is at X_1 and X_2, respectively; and F_{in} is independent of the degree of spinning. F_R appears in the shear flow of the pore passages in the spinning head and is caused by the viscoelasticity normal stress passed by the winding equipment. This was determined by the rheological behavior of the spinning liquid, the flow condition when the spinning head was being passed, and the reeling velocity (V_L):

$$F_R = \pi R_0^2 P^0_{xx,0} \tag{9}$$

The fiction resistance (F_f) refers to the skin fiction force of the spinning dope and the surrounding medium, and its expression is

$$F_f = \frac{2\pi(L - L_0)v^2 C_f}{2g} \tag{10}$$

where v is the velocity and C_f is the coefficient of the friction resistance. This is related to the Reynolds criterion:

$$\begin{aligned} C_f &= 0.68 \times R_e^{-8} \\ R_e &= \frac{Dv\rho^0}{\mu} \end{aligned} \tag{11}$$

where D is the external diameter of the spinning dope, ρ^0 is the medium density, and μ is the medium viscosity. The following equation was obtained when eq. (11) was substituted into eq. (10):

$$F_f = \frac{0.68}{2^{0.2}\,g}(L - L_0)\pi R_L^{0.2}\,\rho^{0^{-0.8}}\,V_L^{1.2}\mu^{0.8} \tag{12}$$

Equation (12) shows that the fiction resistance not only will increase to the 1.2 power of the reeling velocity but also has a relationship with the spinning line and the semidiameter of the spinning trick. F_s on the spinning dope is so little that it can be ignored, and then eq. (5) is transformed to the following expression when F_s is ignored:

$$F_t = F_R + F_{in} + F_f - F_g \tag{13}$$

In eq. (13), only the fiction resistance term and the gravity term are related to the spinning line. Combining F_f with F_g, we obtained the following equation:

$$\begin{aligned} F_f - F_g &= (L - L_0) \\ &\times \left[\frac{0.68}{2^{0.2}}\pi R_L^{0.2}\rho^{0^{-0.8}}V_L^{1.2}\mu^{0.8} - g\pi R_L^2\left(1 - \frac{\rho^0}{\rho}\right)\cos\omega\right] \end{aligned} \tag{14}$$

On the basis of eq. (14), when the fiction resistance is greater than the gravity, that is,

$$\left[\frac{0.68}{2^{0.2}}\pi R_L^{0.2}\rho^{0^{-0.8}}V_L^{1.2}\mu^{0.8} - g\pi R_L^2\left(1 - \frac{\rho^0}{\rho}\right)\cos\omega\right] > 0 \tag{15}$$

the spinning rate is high, and with the increase in the dry-spinning line, the distance ($L - L_0$) between point

TABLE IX
Effects of the Dry-Spinning Distance on the Structure of the Hollow-Fiber Affinity Membrane

Dry-spinning distance (cm)	External diameter (mm)	Wall thickness (mm)	Water flux (L/m^2 h)	Pore diameter (nm)	Porosity (%)
10	1.25	0.27	121.3	39.4	64.0
20	1.20	0.24	141.4	44.2	66.2
30	1.14	0.20	161.5	50.1	69.4

The extrusion volume outflow was 20.4 mL, the additive was PEG (molecular weight = 10,000), the PEG concentration was 4%, the coagulating bath temperature was 25°C, and the ultrafiltration pressure was 0.1 MPa.

L and the spinning head will increase, and the right-hand-side term of eq. (13) will increase. When the reeling velocity is constant, the left term F_t will be invariable. Therefore, to keep the stress balance of the spinning dope, that is, to set up eq. (13), F_{in} and F_R must be reduced. Equation (8) shows that the decrease in F_{in} will result in the decrease in the movement velocity of the spinning dope. From the equation of continuity, we know that the decrease in the movement velocity of the spinning dope will enlarge the cross section of the spinning dope; that is, the wall thickness of the spinning dope will increase, and the inside diameter of the spinning dope will be invariable with the constant flux of the core liquid. Therefore, when the spinning rate is large, the movement velocity of the spinning dope will decrease, and the semidiameter of the spinning dope will increase with the increase in the dry-spinning line. When the friction resistance is less than the gravity, that is,

$$\left[\frac{0.68}{2^{0.2}}\pi R_L^{0.2}\rho^{0^{-0.8}}V_L^{1.2}\mu^{0.8} - g\pi R_L^2\left(1-\frac{\rho^0}{\rho}\right)\cos\omega\right] < 0,$$

the spinning rate is less at this point, and the left-hand-side term F_t of eq. (13) will decrease with the increase in the spinning line. When the reeling velocity is constant, F_t will be invariable, that is, when eq. (13) is set up, F_{in} and F_R must be enlarged. Equation (8) shows that the increase in F_{in} will result in the increase in the movement velocity of the spinning dope. Table IX shows the change in the structure of the hollow-fiber membrane with the change in the length of the dry-spinning line at the constant reeling speed. The flux, pore size, and porosity of the hollow-fiber membrane increased with the increase in the dry-spinning line, but the external diameter and the wall thickness decreased. The change in the dry-spinning line affected the force on the spinning dope; therefore, it resulted in the change in the shape of the spinning dope and then in the change of the external diameter and wall thickness of the hollow-fiber membrane.

Figure 6 presents SEM images of the cross sections of the hollow-fiber membrane in different dry-spinning lines. Under the conditions of continuity, the increase in the movement velocity of the spinning dope will result in a decrease in the cross section of the spinning dope; that is, the external diameter of the spinning dope will decrease. Thus, when the reeling velocity is lower, with an increase in the dry-spinning line, the movement velocity will increase, and the semidiameter of the spinning dope will decrease. In this study, with the increase in the dry-spinning line,

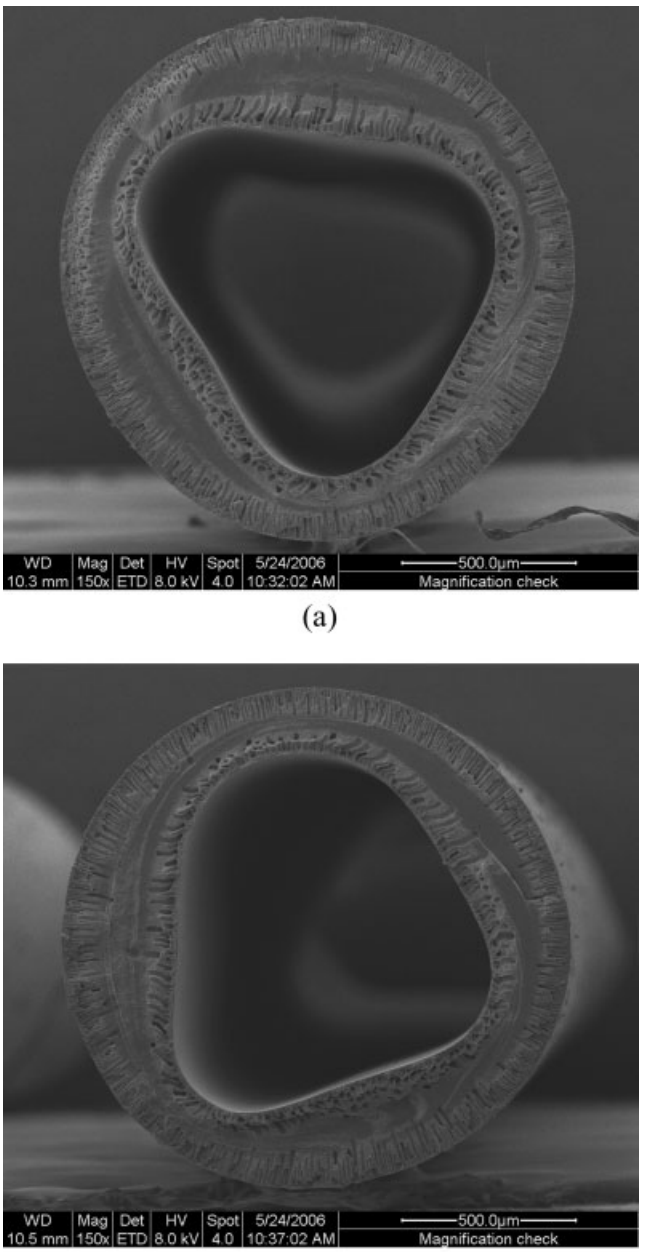

Figure 6 ESEM of the cross section of the hollow-fiber affinity membrane with different dry-spinning distances: (a) 10 and (b) 30 cm.

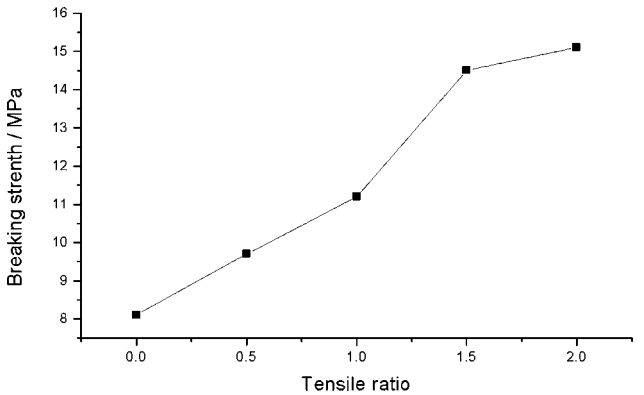

Figure 7 Effects of the tensile ratio on the breaking strength of the hollow-fiber affinity membrane. The tensile temperature was 35°C.

the velocity of the spinning dope increased, the diameter of the spinning dope decreased, the internal diameter was invariable, and the wall thickness decreased. These results agree with the second situation discussed previously. Therefore, the spinning process in this study belongs to the low-velocity spinning process. Because the wall thickness of the spinning dope became thinner with the increase in the dry-spinning line, the diffusional resistance of the solvent decreased and the residence time of the spinning dope in air increased, and the solvent in the spinning dope diffused into the core liquid. This led to the rich phase of PSF in the membrane center moving to the external surface, and then, the thickness of the skin layer and density of the membrane increased; however, because of the fast solvent diffusion and low polymer concentration, the membrane beneath the skin layer formed many big, interconnected, fingerlike pores, the osmotic resistance was reduced greatly, and the porosity and pore size were elevated. In addition, the solvent volatilization could make the membrane surface compact, but DMAc so easily absorbed the moisture in air that the coagulating concentration of the surface layer decreased and the coagulating course changed from total, wet double diffusion to gas-phase coagulation partly. This resulted in the increase in the flux with the increase in the dry-spinning line.

Effects of heat drafting on the mechanical properties of the hollow-fiber affinity membrane

Figures 7 and 8 show the effects of the heat drafting multiple on the breaking strength and breaking elongation of the hollow-fiber membrane, respectively. Figure 7 shows that with the increase in the drafting multiple, the breaking strength of the hollow-fiber membrane increased. The degree of orientation of the PSF macromolecule increased in the axial direction of the hollow fiber, and the heat drafting could increase the breaking strength in the axial direction of the hollow fiber. Figure 8 shows that with the increase in the drafting multiple, the breaking elongation of the hollow-fiber membrane decreased correspondingly. In the drafting process, the degree of orientation of the PSF macromolecule increased in the axial direction of the hollow fiber with the increase in the drafting multiple, the array in the PSF macromolecule fiber became neater, and the texturing capacity of the macromolecular chain decreased. Therefore, the flexibility and breaking elongation of the hollow-fiber membrane decreased under the high-power drafting.

Effects of heat drafting on the structure of the hollow-fiber affinity membrane

The hollow-fiber affinity membrane needed to be heat-drafted to obtain some mechanical properties. The as-formed hollow-fiber membrane was dipped in a liquid bath at a given temperature and was drafted by the tension produced by the rate difference of the two lead rollers. Table X shows the effects of the drafting multiple on the structure of the hollow-fiber membrane. With an increase in the drafting multiple, the flux, pore size, and porosity of the hollow-fiber membrane decreased. The reason is that when the hollow-fiber membrane was drafted above the second-order transition temperature, the random PSF macromolecule chains were tropic in the axial direction of the hollow fiber, then the pore structure of the compact layer and the loose layer were drafted slightly, and the pore size and porosity decreased; therefore, the flux decreased. Drafting with too large a drafting multiple is not appropriate to keep the necessary flux, pore size, and porosity of the hollow-fiber membrane. It is enough to make the hollow-fiber membrane have enough mechanical strength when the drafting multiple is 1–2. Table XI shows the effect of the drafting temperature on the structure of the hollow-fiber membrane under constant drafting conditions. With the increase in the drafting temperature, the flux, pore

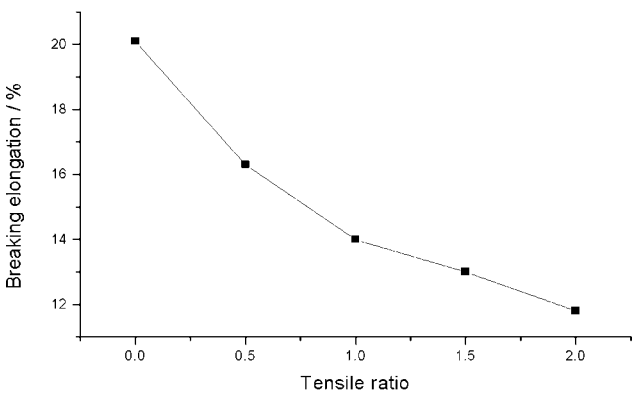

Figure 8 Effects of the tensile ratio on the breaking elongation of the hollow-fiber affinity membrane. The tensile temperature was 35°C.

TABLE X
Effects of the Tensile Ratio on the Structure of the Hollow-Fiber Affinity membrane

Tensile ratio	External diameter (mm)	Inner diameter (mm)	Wall thickness (mm)	Water flux (L/m^2 h)	Pore diameter (nm)	Porosity (%)
0.0	1.25	0.68	0.28	121.3	39.1	64.0
0.5	1.20	0.62	0.26	117.2	38.2	63.1
1.0	1.18	0.58	0.22	111.3	36.6	61.2
1.5	1.16	0.56	0.20	105.4	35.0	59.2
2.0	1.13	0.52	0.19	103.2	34.2	58.4

The tensile temperature was 30°C, the extrusion volume outflow was 20.4 mL, the additive was PEG (molecular weight = 10,000), the PEG concentration was 4%, the coagulating bath temperature was 25°C, and the ultrafiltration pressure was 0.1 MPa.

size, and porosity of the hollow-fiber membrane decreased. With the increase in the drafting temperature, the PSF macromolecule chains were easier to move, and the moving ability of the macromolecule chains was stronger. In the drafting process of the hollow-fiber membrane at a higher temperature, the PSF macromolecules more easily became tropic in the axial direction of the hollow fiber, then the pore structure of the compact layer and the loose layer were drafted slightly, and the pore size and porosity decreased.

Effects of the heat treatment on the structure of the hollow-fiber affinity membrane

The objective of the heat treatment is to elevate the homogeneity and stability of structure of the hollow-fiber membrane. There are three factors that affect the membrane structure in the process of the heat treatment: the temperature of the heat treatment, the medium of the heat treatment, and the time of the heat treatment. The effect of the temperature of the heat treatment on the membrane structure is the most appreciable. Table XII shows the effects of the heat treatment of the hollow-fiber affinity membrane at different temperatures in the same medium and for the same time of the heat treatment. The flux, pore size, and porosity of the hollow-fiber membrane decreased with the increase in the heat-treatment temperature. With the increase in the heat-treatment temperature, the fiber membrane became compact, and that resulted in the decrease of the flux. The pore size compacted too much, so the flux decreased seriously when the temperature was over 55°C. Therefore, the temperature of the heat treatment should be controlled from about room temperature to 35°C for the hollow-fiber affinity membrane.

CONCLUSIONS

Our investigation has proved that blends of a mercapto chelating resin and PSF can be used to prepare high-quality, heterogeneous hollow-fiber affinity membranes. Several processing parameters, such as the mass ratio of the mercapto chelating resin to PSF in the casting solution, the size of the mercapto chelating resin, the PSF content, the additive content, and the temperature of the casting solution, have significant effects on the structure of the heterogeneous hollow-fiber affinity membrane modified with the mercapto chelating resin. The external diameter, wall thickness, and porosity of the hollow-fiber affinity membrane increase with an increase in the extrusion volume rate when other spinning parameters are constant, but the pore size and the flux decrease. Too high a flux of the core liquid is adverse to improving the

TABLE XI
Effects of the Tensile Temperature on the Structure of the Hollow-Fiber Affinity Membrane

Tensile temperature (°C)	Water flux (L/m^2 h)	Pore diameter (nm)	Porosity (%)
25	110.2	36.4	61.3
35	104.3	33.3	58.4
45	95.2	31.4	52.3

The tensile ratio was 1, the additive was PEG (molecular weight = 10,000), the PEG concentration was 4%, the casting solution temperature was 25°C, the coagulating bath temperature was 25°C, and the ultrafiltration pressure was 0.1 MPa.

TABLE XII
Effects of the Thermal-Treatment Temperature on the Structure of the Hollow-Fiber Affinity Membrane

Thermal-treatment temperature (°C)	Water flux (L/m^2 h)	Pore diameter (nm)	Porosity (%)
25	109.5	35.2	59.3
35	102.8	32.3	57.4
45	93.4	29.4	51.5
55	50.1	22.6	42.7

The thermal-treatment medium was water, the thermal-treatment time was 5 h, the additive was PEG (molecular weight = 10,000), the PEG concentration was 4%, the casting solution temperature was 25°C, the coagulating bath temperature was 25°C, and the ultrafiltration pressure was 0.1 MPa.

membrane performance. The asymmetric structure of the hollow-fiber affinity membrane has a close relationship with the diffusion difference of the solvent in the dry- and wet-spinning line phases. The hollow-fiber affinity membrane needs to be heat-drafted to obtain some mechanical strength. However, the heat drafting decreases the flux, pore size, and porosity of the hollow-fiber membrane. In general, the hollow-fiber affinity membrane can not only obtain enough mechanical strength but also keep an appropriate pore size, porosity, and flux when the drafting multiple is 1–2. Finally, the heterogeneous hollow-fiber affinity membrane modified with a mercapto chelating resin should have a tension heat-set to increase the homogeneity and stability of the structure.

References

1. Wang, B.; Huang, W.; Yang, X. J Appl Polym Sci 2005, 93, 990.
2. Serfica, G. C.; Pimbley, J.; Belfort, G. J Membr Sci 1994, 88, 292.
3. Costello, M. J.; Fane, A. G.; Hogan, P. A.; Ruckenstei, E.; Guo, W. J Membr Sci 1993, 80, 131.
4. Wang, B.; Cui, Y.; Du, Q.; Pei, G. J Dong Hua Univ (Engl Ed) 2002, 19, 49.
5. Wickramasinghe, S. R.; Semments, M. J.; Cussler, E. L. J Membr Sci 1993, 84, 1.
6. Hawkins, D. M.; Trache, A.; Ellis, E. A.; Yang, L.; Hsiao, W.; Chen, P. J Membr Sci 2002, 197, 185.
7. Wang, B.; Cui, Y. F.; Du, Q. Y. J Appl Polym Sci 2003, 87, 908.
8. Gao, Y. X.; Ye, L. B. Base of Membrane Separation Technology; Science Press: Beijing, 1989; p 173.
9. Hirose, S.; Shimizu, A.; Nose, T. J Appl Polym Sci 1979, 23, 3193.
10. Wang, G. H. Principle of Forming and Processing of Polymer Materials; Chemical Industry: Beijing, 1982; p 279.